Two-dimensional plasma plume density characterisation of the IFM Nano Thruster

IEPC-2019-566

Presented at the 36th International Electric Propulsion Conference
University of Vienna, Austria
September 15-20, 2019

Sebastian Keerl,[*] Werner Engel,[†] Nina S. Mühlich,[‡] Johanna Fries,[§] Bernhard Seifert,[¶]
Emre Ceribas,[‖] Robert-Jan Koopmans[**]
FOTEC Forschungs- und Technologietransfer GmbH, Wr. Neustadt, 2700, Austria
and
David Jelem[††]
TTTech Computertechnik AG, Vienna, 1040, Austria

The IFM (Indium FEEP Multi Emitter) Nano Thruster, developed at FOTEC and commercialised by Enpulsion, is a 1U sized FEEP (Field Emission Electric Propulsion) system. It can also be used for precise orbit control of satellites and deep space missions. It consists of a porous tungsten crown ion emitter providing thrust in the range of 10 μN to 0.4 mN at an I_{sp} of 2000 s to 6000 s. To obtain a better understanding of the thruster efficiencies as well as to determine basic thruster characteristics, a detailed plasma field investigation of this thruster is essential. An extensive measurement campaign was conducted in order to map the beam ion current density at a fixed distance from the thruster at different horizontal and vertical angles from the centre line of the thruster. This two-dimensional mapping was achieved by using an array of 23 Faraday cups on a rotating boom. Measurements were performed with a horizontal spatial resolution of 1° and between 4° to 10° in the vertical direction. At each position the ion current was determined by performing a voltage sweep with each of the Faraday cups. The Faraday cups were specifically designed for this task, taking into account the expected low ion density. Each of those probes have a built-in ring repeller with an orifice of 1 cm. As the estimated Debye length of the plasma is on the order of several cm, this repeller can be used as a single hole grid. When biasing negatively, it prevents thermal electrons from entering the Faraday cup. Furthermore, it retains any secondary electrons created inside the Faraday cup. The resulting beam profiles have densities on the order of μA/cm^2 at 95 cm from the emitter. This paper describes the for these plasmas new developed probes in more detail as well as the first ever 2-D density characterisation of the plume of an IFM Nano thruster.

[*]Researcher, Aerospace Engineering, keerl@fotec.at
[†]Researcher, Aerospace Engineering, engel@fotec.at
[‡]Researcher, Aerospace Engineering, muehlich@fotec.at
[§]Researcher, Aerospace Engineering, fries@fotec.at.
[¶]Head of Electric Propulsion, Aerospace Engineering, seifert@fotec.at.
[‖]Researcher, Aerospace Engineering, ceribas@fotec.at
[**]Head of Chemical Propulsion, Aerospace Engineering, koopmans@fotec.at
[††]Junior Product Manager, TTEthernet equipment for Human Space Exploration, david.jelem@gmail.com.

List of abbreviations

$FEEP$	= Field-Emission Electric Propulsion
IFM	= Indium FEEP Multi Emitter
SEE	= Secondary Electron Emission
PCB	= Printed Circuit Board
$PEEK$	= Polyether Ether Ketone
HET	= Hall Effect Thruster

I. Introduction

The IFM Nano Thruster, developed at FOTEC and commercialised by Enpulsion, is a 1U sized FEEP system, that can also be used for precise orbit control of satellites and deep space missions. Indium is used as the propellant, which is in its solid phase during launch of the spacecraft. Once in orbit, it is heated up to above its melting temperature. About 230 g are stored in the thruster tank and in the 28 porous needles of the emitter crown. This crown can be positively biased up to 10 kV and serves as the thruster emitter. A circular ring is mounted around the needle tips of the crown and can be biased up to −10 kV, serving the function of the extractor. This potential difference leads to the formation of a Taylor cone and the expulsion of ions from the liquid indium with an energy equivalent to the emitter potential.[1] The expelled ions bear a certain angular density distribution. The knowledge of this distribution is of high importance to prevent damaging of solar panels and other parts of the satellite during operation.[2] Previously, ion density wire probe measurements were conducted as well as relative ion density measurements with a segmented collector in the plume of an indium FEEP thruster.[3,4] In contrast to the plume measurements of a Hall thruster, the two-dimensional investigation of the plume of an indium FEEP emitter was not performed with the use of Faraday cups before.[5,6]

The paper is strucutred as follows. First, the design of a Faraday cup probe is being described in chapter II. Second, measurements with the Faraday cups were conducted and are being discussed in chapter III. Finally, the conclusion follows in chapter IV.

II. Faraday cup design

A. Design requirements

Low density

The beam of an IFM Nano thruster has a low density on the order of μA/cm^2 at 95 cm from the emitter.[4] For example, in comparison to a Hall Effect Thruster (HET), the ion plume density of a FEEP thruster is on the order of 1×10^5 lower.[4,6] As the Debye length is inversely proportional to the square root of the particle density and the Debye length in the plume of a HET is on the order of 0.1 mm, the Debye length in the plume of the IFM Nano thruster is to be expected on the order of several cm.[7] As the requirement is to place several probes next to each other with distances also in the order of cm for a two-dimensional mapping, planar probes or nude Faraday cups would lead to false measurements as the plasma sheaths of different probes would overlap. Furthermore, the orifice of the probe must be large enough to be able to measure at low densities.

Secondary electron emission

Secondary electron emission is a phenomenon that occurs when ions hit the surface of the probe material. The secondary electron yield was found in a previous FEEP plume diagnostics campaign to be above 1 electron per ion.[3] This entails a wrong measured current of the primary fast beam ions of at least a factor of 2. Therefore, the probe needs to be designed such that the contribution of this phenomenon is suppressed.

Thermal background particles

As there are thermal ions present in the vacuum chamber that could lead to a wrong density reading of the fast ion beam particles, the particle collector needs to be able to be biased to a value above the energy of the thermal ions.

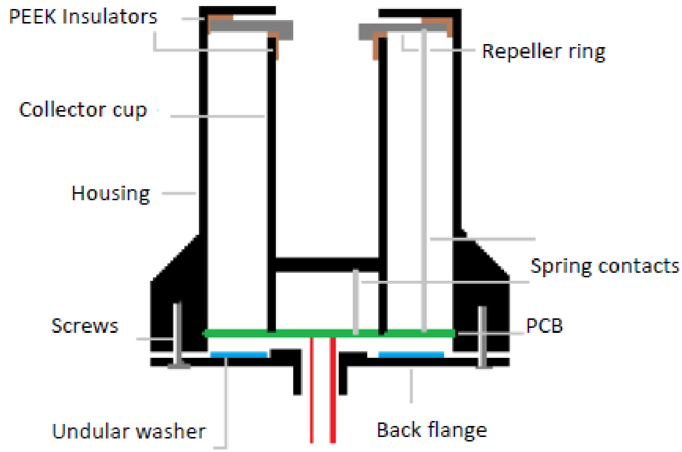

Figure 1: Structural view of the Faraday cup and its components.

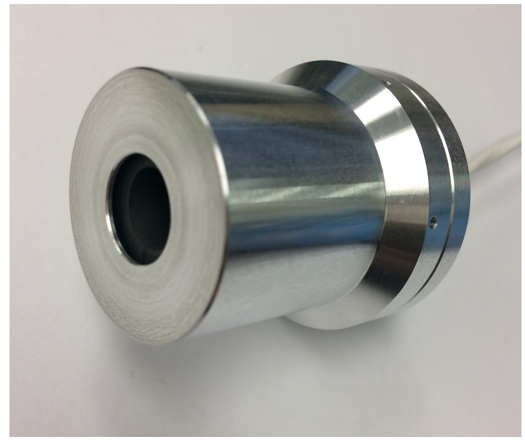

Figure 2: Photograph of the assembled Faraday cup.

Sputtering and deposition effects

A maximum lifetime and minimised maintenance time is required. A probe emerged in the beam is subject to sputtering and deposition effects.[3] Due to the electrical conductivity of the deposited indium, the probe needs to be designed such that the risk of short circuits between independantly biased parts of the probe is minimised. Furthermore, no screws or threads should be directly exposed to the beam as the deposition on these would lead to permanent damage.

B. Design description

Many different designs for Faraday cups exist, from the simple nude model to more complex types.[8]

Figure 1 shows the structural view of the Faraday cup and Fig. 2 a close-up photograph of the assembled Faraday cup. This newly developed Faraday cup design comprises a cup-shaped collector. This ensures that even though the Debye length is on the order of several cm, a distance of a few cm between several probes is possible. The outer aluminium shielding consists of two separate pieces that are held together by six screws. These are located at the rear housing piece and are therefore not subject to indium deposition. This outer shielding also contains the feed-through for a two-line cable; one line for the voltage biasing of the collector cup and one for the biasing of the repeller ring. These electrical lines are soldered to a PCB, which is separated from the rear shielding piece by an undular washer. This ensures that when tightening the six screws at the rear piece, all electrical connections are secured. From this PCB one spring contact pin connects to the collector cup, and one to the repeller ring. This ensures independant biasing of the collector and the repeller. The repeller bias is held constant; on the collector cup, however, a voltage sweep is being performed. When biasing the repeller to negative voltages higher than the equivalent thermal energy of secondary electrons, those electrons can be recaptured within the cup. Furthermore, thermal electrons in the outer vicinity of the cup are being repelled. The repeller ring is made from graphite and has an orifice of 1 cm. Graphite was chosen, as it has a low sputter yield and a low secondary electron coefficient.[9] The collector cup sits countersunk on the PCB. The material for this collector was chosen to be aluminium. Other materials e.g. molybdenum do have a lower electron work function, and therefore less SEE, however the advantage is limited and outweighed by the extra costs. A PEEK cylinder, located at the top of the collector cup acts as an insulator between the cup and repeller. This insulator was dimensioned such that it has a comparatively large surface area to prevent short circuiting due to indium deposition. The repeller ring is electrically disconnected from the outer housing by another PEEK piece. This PEEK ring is well hidden inside the outer housing to create a labyrinth-like structure in order to prevent short circuiting due to indium deposition.

III. Faraday cup measurements

23 Faraday cups of the above described design were manufactured and were mounted on a rotating boom, separated at a vertical angular resolution of 4° to 10°. At each of those cups the repeller can be biased, a voltage sweep on the collector cup performed and the resulting current measured. Measurements were performed at horizontal resolution of 1°.

A. Secondary electron emission and fast beam ions

In order to investigate the suppression of SEE, one Faraday cup was positioned on the thruster axis line at a vertical and horizontal angle of 0° at a distance of 95 cm from the emitter ($I_{Em} = 2\,\mathrm{mA}$, $U_{Em} = 6\,\mathrm{kV}$, $U_{Ex} = -3.5\,\mathrm{kV}$). Then, voltage sweeps were performed at different repeller biases. Figure 3 shows the current density j as a function of the cup collector voltage U_{cup}. U_{cup} was swept in 1 V steps from −100 V to 100 V. This was repeated for the following different repeller voltages U_{rep}: 30 V, 15 V, 2 V, −5 V, −10 V and −20 V.

The symbols indicate raw data points. For better visibility, a Savitzky-Golay smoothing filter (window length=37, polynomial order=2) was used, which is shown as solid lines. All of the curves show an increase from −100 V probe bias to around −25 V. A steeper increase in current density is visible for U_{cup} between −25 V and 0 V. The higher U_{rep}, the steeper this increase is. At a collector bias between 0 V and 75 V and a negative U_{rep} the current density remains constant at about $-0.10\,\frac{\mu\mathrm{A}}{\mathrm{cm}^2}$. All of the curves intersect at around 4 V. To the right of this point the highest current density is recorded for the repeller ring with the highest positive ring bias. Below a U_{rep} of −5 V the curves above U_{cup} of roughly 4 V stay constant. This could indicate the suppression of the secondary electrons with an energy lower than 5 eV. Therefor, a bias of $U_{rep} = -15\,\mathrm{V}$ was chosen in the following, being well below the electron suppression voltage of −5 V.

Figure 4 shows the influence of different sources to the recorded current density. Four main contributors to this current density were identified:

$$j_{tot} = j_{ion,fast} + j_{SEE} + j_{ion,therm.} + j_{e,therm.} \tag{1}$$

The blue curve ($U_{rep} = 30\,\mathrm{V}$) and the red curve ($U_{rep} = -10\,\mathrm{V}$) increase in total current with higher U_{cup} between $U_{cup} = -80\,\mathrm{V}$ and $U_{cup} = -20\,\mathrm{V}$. The fast beam ions $j_{ion,fast}$ provide a constant contribution independant of U_{cup}. In this region the secondary electrons, resulting from the impact of fast beam ions, can not be recaptured by the Faraday cup; U_{cup} is much larger than the equivalent thermal energy of these secondary electrons. Therefore, these electrons increase the total measured current as missing electrons in the probe, denoted as j_{SEE}. Thermal ions $j_{ion,therm.}$, which are present in the vacuum chamber, increase the total current as well. However, in comparison to the other two factors, $j_{ion,fast}$ and j_{SEE}, this thermal ion contribution is not constant but increases with higher negative U_{cup}. This is the case for both U_{rep} biases. The thermal electrons $j_{e,therm.}$ in the vicinity of the cup do not contribute to the red curve due to the negatively biased repeller ring. They do contribute to the blue curve above $U_{cup} = -30\,\mathrm{V}$ and therefore contribute to the measured total current for $U_{cup} > 0\,\mathrm{V}$. The red curve, however, where the outer thermal electrons are repelled by $U_{rep} = -10\,\mathrm{V}$, secondary electrons recaptured and thermal ions repelled by $U_{cup} > 0\,\mathrm{V}$ it is assumed that only the fast beam ions contribute to the measured current. Hence, the red curve at voltages roughly higher than $U_{cup} \sim 0\,\mathrm{V}$ is presumed to be the correct fast ion beam current.

B. Beam profile

For the calculation of the 1-D beam ion density profile a mean value for $j_{ion,fast}$ between U_{cup} of 30 V and 40 V was used. This was done to smooth the data points. The repeller ring was set to −15 V. In order to obtain a 1-D beam ion density profile, data was recorded with the Faraday cup at the position corresponding to a vertical angle of 0°, while rotating the boom from −80° to 80° with a step size of 1°. Figure 5(a) shows such a 1-D beam profile. The red dots denote the raw data points, the solid line is the result of a Savitzky-Golay smoothing filter (window length=31, polynomial order=3). The thruster parameters were set to $I_{Em} = 3\,\mathrm{mA}$, $U_{Em} = 6\,\mathrm{kV}$, $U_{Ex} = -5.1\,\mathrm{kV}$. There were 27 firing needles and the background pressure was at about 1×10^{-7} mbar. The curve shows an increase from −80° to about −15°. However, a wing-like shape between about −70° and −45° is visible. At around −15° the slope decreases and the red line reaches its maximum at around 15°. After that, a current density decrease sets in until 80°. Again, between roughly 45° and 55° a wing-like shape is visible.

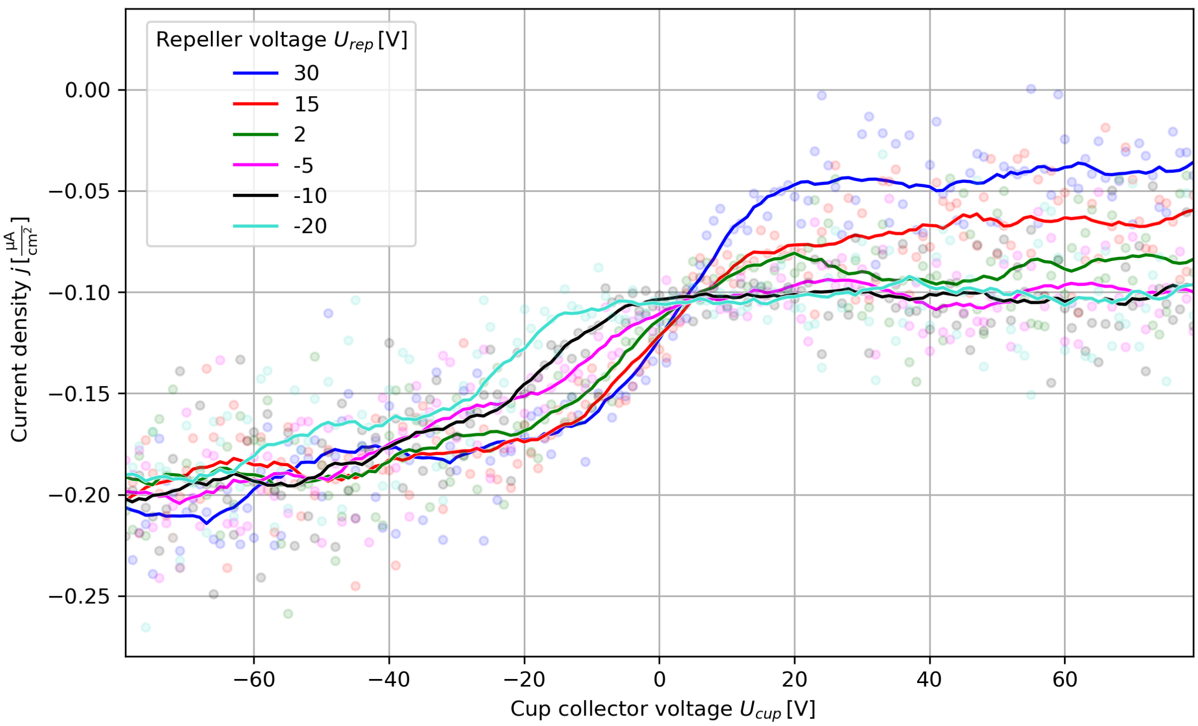

Figure 3: Current density as a function of cup collector voltage at various repeller voltages. Data recorded with a Faraday cup at vertical and horizontal angles of 0°.

The influence of the background pressure on the measurements is shown in fig. 5(b): 5×10^{-7} mbar (red), 5×10^{-6} mbar (blue) and 5×10^{-5} mbar (green). The beam profiles were recorded at constant thruster parameters ($I_{Em} = 2$ mA, $U_{Em} = 6$ kV, $U_{Ex} = -3.5$ kV, 27 firing needles). Only at pressures higher than 5×10^{-6} mbar (blue) an effect can be seen. The green curve stays below the other two over the entire angle range. Therefore, it is assumed that below 1×10^{-6} mbar the background pressure only has a minimal influence on the ion density measurement.

For the 2-D beam ion density presentation, all 23 Faraday cups were used. The thruster parameters were held stable at $I_{Em} = 3$ mA, $U_{Em} = 6$ kV, $U_{Ex} = -5.1$ kV with 27 needles firing. The pressure was on the order of 1×10^{-7} mbar. Data of all 23 Faraday cups were recorded for every 1° step of the boom. Figure 6 shows the two-dimensional fast beam ion current density. The x-axis denotes the horizontal angle θ, defined by the 1° steps of the boom, the y-axis denotes the vertical angle ϕ of each Faraday cup position. For the calculation of the ion density a mean value for $j_{ion,fast}$ between U_{cup} of 30 V and 40 V was used. The repeller ring was set to −15 V. The maximum at around 0.12 µA/cm^2 is represented by bright yellow, the minimum by black. Dark purple cells (∼0.01 µA/cm^2) start to show up at angles of roughly −70° and 70° in both angles. Between −60° and −40° and between 40° and 60° the current density increases from purple (∼0.02 µA/cm^2) to the transition of purple and red (∼0.05 µA/cm^2). A steep increase in ion density, from ∼0.05 µA/cm^2 to ∼0.09 µA/cm^2 can be seen between −40° and −20° and between 20° and 40° in both angles. The center (−15° to 15°) shows a plateau-like structure at around 0.11 µA/cm^2 to 0.12 µA/cm^2, denoted by bright yellow. All in all, the profile seems to be relatively uniform over the horizontal and vertical axis.

IV. Conclusion

This paper describes the development of a device that is capable of measuring a directed plasma beam at low densities. This device is built such that it can be easily implemented onto the rotating boom and has a substantial lifetime. With the cup-shaped structure and the built-in repeller it is possible to suppress the

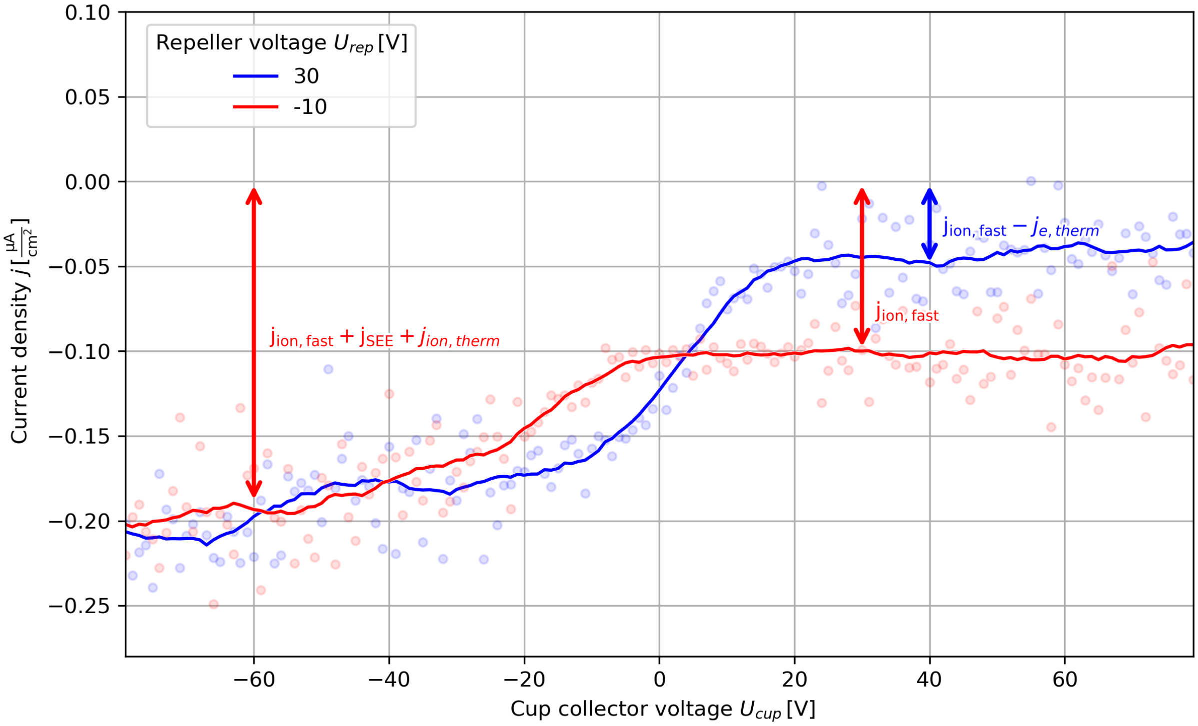

Figure 4: Current density as a function of cup collector voltage at various repeller voltages. Data recorded with a Faraday cup at vertical and horizontal angles of 0°.

contribution of SEE and then to determine the fast beam ions. Not only in one dimensions but also in two dimensions while using all 23 Faraday cups simultaneously, leading to the first-ever recorded 2-D ion beam density representation of an IFM Nano device. It was shown that at pressures below 5×10^{-6} mbar there is no significant influence on the measurement from any background particles. The 2-D beam ion density showed a quite uniform thruster beam ion density with a maximum of around $0.12\,\mu A/cm^2$.

Acknowledgments

The research leading to the results was supported by the ESA project ‘IFM Nano Thruster Module‘, contract number 4000116898/16/NL/EM under the ARTES 5.2 programme framework.

In addition, the first author would like to thank Dr. Stéphane Mazouffre for the very helpful discussion during the design phase of the beam diagnostics setup.

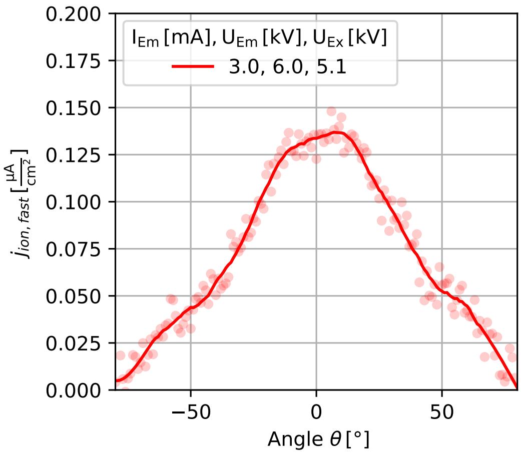

(a) Fast ion beam density as a function of horizontal angle recorded with the Faraday cup at the position corresponding to a vertical angle of 0°.

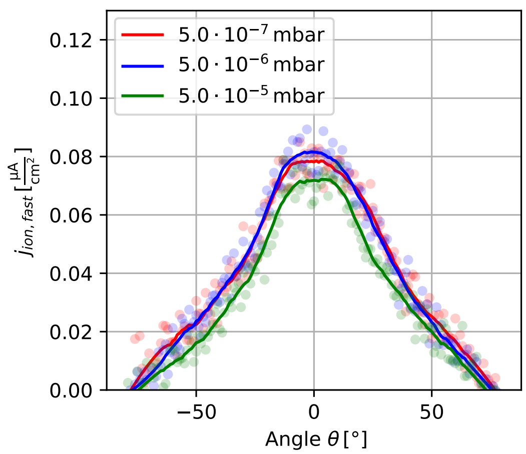

(b) Fast ion beam density as a function of horizontal angle recorded with the Faraday cup at the position corresponding to a vertical angle of 0° for three different background pressures.

Figure 5: 1-D beam ion density profiles of an IFM Nano thruster.

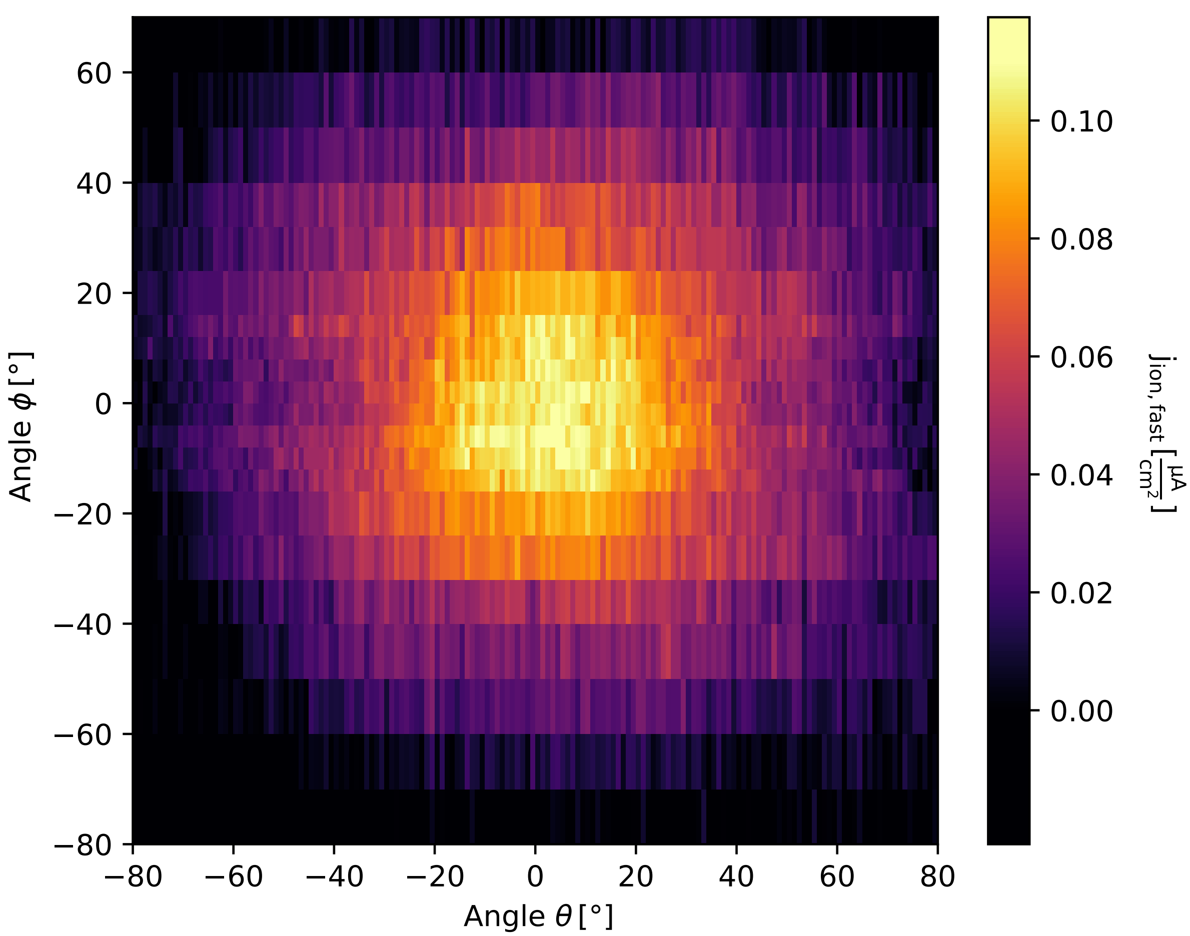

Figure 6: 2-D beam ion density profile of an IFM Nano thruster at a distance of 95 cm from the emitter.

References

[1]Richard G. Forbes and Neboysha N. Ljepojevic. Liquid-metal ion source theory: electrohydrodynamics and emitter shape. *Surface Science*, 266(1):170 – 175, 1992.

[2]Lyon B. King and Alec D. Gallimore. Ion-energy diagnostics in the plasma exhaust plume of a hall thruster. *Journal of Propulsion and Power*, 16(5):916–922, 2000.

[3]M. Tajmar, K. Marhold, and S. Kropatschek. Three-dimensional In-FEEP plasmadiagnostics. In *Proceedings of the 28th International Electric Propulsion Conference*, IEPC-03-161, Toulouse, France, 2003.

[4]David Jelem, Alexander Reissner, Bernhard Seifert, Nembo Buldrini, Lissa Wilding, and David Krejci. Direct thrust and plume divergence measurements of the ifm nano thruster. *Advances in Space Research*, 62(12):3398 – 3404, 2018. Advances in Technologies, Missions and Applications of Small Satellites.

[5]Joshua L. Rovey, Mitchell L. R. Walker, Alec D. Gallimore, and Peter Y. Peterson. Magnetically filtered faraday probe for measuring the ion current density profile of a hall thruster. *Review of Scientific Instruments*, 77(1):013503, 2006.

[6]David Manzella and John Sankovic. *Hall thruster ion beam characterization.*

[7]Colleen M Marrese, Neha Majumdar, J Haas, George Williams, LB King, and Alec D Gallimore. Development of a single-orifice retarding potential analyzer for hall thruster plume characterization. In *25th International Electric Propulsion Conference. IEPC-97-066; Cleveland, OH*, pages 397–404, 1997.

[8]Daniel L. Brown and Alec D. Gallimore. Evaluation of ion collection area in faraday probes. *Review of Scientific Instruments*, 81(6):063504, 2010.

[9]D. Pagano, F. Scortecci, C. Bundemann, C. Eichhorn, F. Scholze, H. Neumann, H.J. Leiter, H. Kersten, S. Gauter, R. Wiese, R. Blott, P.J. Klar, K. Holste, B. Meyer, S. Mazouffre, A. Bulit, and J. Gonzales del Amo. Qualification of the AEPD System as a Standard On-Ground Tool for Electric Propulsion Thruster. IEPC-2015-363, Hyogo-Kobe, Japan, July 2015.